[10]M. E. Rudd, T. Jorgensen, Jr., and D. J. Volz, Phys. Rev. Lett. **16**, 929 (1966).
[11]S. Ormonde, J. McEwen, and J. W. McGowan, Phys. Rev. Lett. **22**, 1165 (1969).
[12]L. Sanche and P. D. Burrow, Phys. Rev. Lett. **29**, 1639 (1972).
[13]R. E. Huffman, J. C. Larrabee, and U. Tanaka, J. Chem. Phys. **46**, 2213 (1967).
[14]L. M. Branscomb, D. S. Burch, S. J. Smith, and S. Geltman, Phys. Rev. **111**, 505 (1958).
[15]Hugh Kelly (private communication).

PHYSICAL REVIEW A VOLUME 8, NUMBER 1 JULY 1973

Photon-Particle Coincidence Measurement of Charge-Transfer Excitation of the N_2^+ First Negative 3914-Å Band by Protons*

P. J. Wehrenberg and K. C. Clark
Department of Physics, University of Washington, Seattle, Washington 98195
(Received 22 January 1973)

The cross section for charge-transfer excitation of the N_2^+ first negative 3914-Å band by protons (5–65 keV) has been measured using a photon-particle coincidence technique. The target N_2 is collisionally excited to the N_2^+ ($B^2\Sigma_u^+$) state and emits a 3914-Å photon in the (0,0) transition. This photon is detected in coincidence with the scattered particle, a proton or hydrogen atom, allowing separation of the two reactions which contribute to 3914-Å emission. The cross section for charge-transfer excitation indicates that charge transfer is the dominant contributor to 3914-Å excitation at energies below 10 keV, and that ionization with excitation becomes increasingly important with increasing energy. The by-product measurements, which include the cross section for charge transfer, the total cross section for 3914-Å emission, and the lifetime of the N_2^+ ($B^2\Sigma_u^+$) state, agree well with those of other workers.

I. INTRODUCTION

The excitation of the $B^2\Sigma_u^+$-$X^2\Sigma_g^+$ (0,0) emission of N_2^+ by protons of 5–65-keV energies has been studied by use of a coincidence technique. Specifically, photons emitted in the predominant (0,0) band at 3914 Å are detected in coincidence with the fast scattered proton or hydrogen atom. Because the experiment determines the final charge state of the exciting particle in an individual collision, two possible processes of ionization with excitation are separately measurable.

Protons incident on N_2 can participate in two reactions, both of which can produce the same band emission. A charge exchange can occur, leaving the N_2^+ ion in an excited state which subsequently emits a 3914-Å photon. Alternatively, the proton can excite and ionize the molecule without picking up the electron. In standard experiments the total fluxes of photons and of particles are measured, and there is no way to correlate the excitation of the N_2^+ ion with a charge-exchange collision. However, this present study of the time-interval spectrum between photons and scattered particles allows the competing reactions to be studied independently.

In addition to the measurement of the charge-exchange excitation cross section, it is possible to measure the total charge-exchange cross section, the total excitation cross section, and the lifetime of the $B^2\Sigma_u^+$ level of N_2^+. The charge-exchange and excitation cross sections have been studied by many workers; reviews of measurements and some new work have recently been presented by deHeer,[1,2] and by McNeal and Birely.[3]

Recent experiments by Jaecks, Crandall, and McKnight[4] have used an atom-photon coincidence technique to study differential cross sections for capture into excited states in $H^+ + He$ collisions. They detect photons from the neutralized H atom in coincidence with the atom itself. An ion-photon coincidence technique has been used by Barat and co-workers[5] to investigate the differential cross section for excitation of the 3^3P level in He by He^+ ions. Both of these experiments use relatively large ($\simeq 7°$) scattering angles, infer impact parameters through the quantity $\tau = E\theta$, and analyze their data in terms of level crossings.

In the experiment described here detection of the fast beam particle can be differential in angle or integrated over a forward-scattering cone which intercepts most of the scattered incident particles. The data presented here were taken using the large angular acceptance mode to define charge states of the primary reactants.

The application of coincidence techniques in analysis of the products of atomic collisions is a relatively recent development. The original work of Afrosimov, Gordeev, Panov, and Fedorenko[6] detected the principal reactants in $Ar^+ + Ar$ collisions, and very similar techniques were developed independently by Kessel and Everhart.[7] Bingham[8]

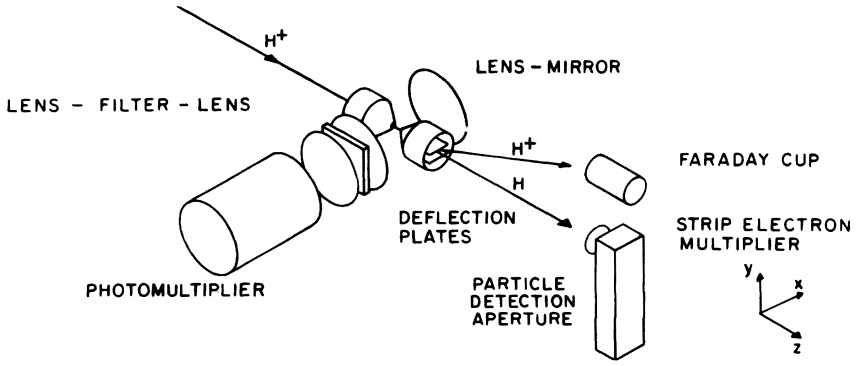

FIG. 1. Schematic diagram of experiment.

has also used particle-particle coincidence. As optical photon detection efficiencies have improved, photon-photon and particle-photon coincidence experiments have become possible. Young, Murray, and Sheridan[9] have used Balmer α and 3914-Å photons from protons on N_2. The development of various types of photon-particle coincidence experiments is reported by Jaecks, by Barat, and in this paper.

II. EXPERIMENTAL CONSIDERATIONS

A. Measurement of Coincidence Cross Section

The collision region and detector arrangement are shown in Fig. 1. A low-current beam of protons from a dc ion source is accelerated, focused, mass selected, collimated within ±1.5 mrad, and passed through a differentially pumped collision region 1 cm in length containing thermal N_2. Details of the dc ion source, accelerator, photon detector, particle detector, and electronics will be published elsewhere.

Photons from the collision region are collected by a fast optical system, transmitted by a 3914-Å interference filter, and focused on the cathode of a cooled photomultiplier. The anode circuit and subsequent electronics allow counting of pulses arising from single photons with 2-ns time resolution.

The incident fast particle continues to drift 32 cm farther and is detected by a Bendix strip electron multiplier (SEM). The charged beam, containing unscattered and scattered protons, is separated from the neutralized beam by electrostatic deflection into a displaced Faraday cup. The beam current is integrated to a selected value of charge, and the discriminators in the particle, photon, and clock channels are then gated off. The integrated beam current, in conjunction with monitored target pressure, is used for normalization at various energies.

The circular aperture at the detector, shown in Fig. 1, defines the angle of scattering with respect to the collision region. This cylindrical symmetry eliminates any angular dependence on the angle of rotation about the beam axis.

The time-interval spectrum is acquired by starting a time-to-amplitude converter (TAC) with a photon-initiated pulse, and stopping the converter with a particle-initiated pulse. The TAC output is then processed by a multichannel analyzer, which accumulates the total number of coincidences over the period P of a data run, approximately 10^3 s.

The number of true coincidences n_T observed in a data run is related to the cross section through the following equation:

$$n_T = \int^{\Delta\Omega_p} \int^{\Delta\Omega_\lambda} \frac{\partial^2\sigma_{p\lambda}}{\partial\Omega_p \partial\Omega_\lambda}\, d\Omega_p\, d\Omega_\lambda\, \epsilon_\lambda \epsilon_p G \times \frac{1}{\tau_\lambda} \int_{t_d}^{t_d+t_r} e^{-t/\tau_\lambda}\, dt \int_0^P I\mu l\, dt' . \quad (2.1)$$

The various factors in this expression are now considered. The cross section for the reaction $H^+ + N_2 \rightarrow p + (N_2^+) + h\nu\,(\lambda = 3914\ \text{Å})$ with photon emission into the solid angle $d\Omega_\lambda$ and particle scattering into $d\Omega_p$ is represented by $\partial^2\sigma_{p\lambda}/\partial\Omega_p\partial\Omega_\lambda$. The particle detector and photon detector intercept solid angles $\Delta\Omega_p$ and $\Delta\Omega_\lambda$, respectively. The efficiency for detecting photons of wavelength λ and the efficiency for detecting the particle p at an energy E are given by ϵ_λ and ϵ_p, respectively. The efficiencies for both protons and hydrogen atoms vary as a function of kinetic energy. The factor giving the overlap integral of the viewing regions of the two detectors is represented by the symbol G. The third integral accounts for the fact that the lifetime of the excited state is long compared to the resolving time, where τ_λ is the lifetime characteristic of the excited level. The time delay introduced by postcollision drift of the particle and instrumental delays and the resolving time of the coincidence apparatus are represented by t_d and t_r, respectively.

The fourth integral accounts for variations in beam current and target density during the period of a data run. There are, however, restrictions

on the allowable time dependence of the beam current. These are discussed in Sec. IV C.

The fourth integrand is the product of beam current, target density, and collision-region length. In general, this integrand is a function of time. The target pressure was monitored during all data runs and varied less than 0.4%/h; therefore electronic multiplication of I and μ was not considered necessary in normalization. The runs were then normalized to an electronically integrated value of beam charge, $Q = \int_0^t I dt'$.

Some of the factors in Eq. (2.1) can be simplified or avoided by apparatus design and data analysis. The factor G, which represents the overlap integral of the regions viewed by the two detectors, is equal to unity if both detectors always observe the entire interaction region with uniform efficiency. For the collision cell and detector geometry used here, the particle detector views the entire collision region regardless of angle because the exit orifice of the collision region is larger than the maximum scattering cone subtended by the particle detector and collision-cell entrance orifice.

A related requirement is that the excited molecular ions have not drifted out of the photon detector field of view before emitting. This requirement can be stated as

$$\frac{\text{radius of field of view}}{\text{maximum speed of } (N_2^+)^*} \gg \tau_\lambda . \tag{2.2}$$

For the extreme case of 1.2° scattering of a 65-keV proton this ratio has the value $29\tau_\lambda$, and the inequality is satisfied. The maximum Doppler shift of emission from the resulting $(N_2^+)^*$ is 0.07 Å, which is negligible relative to the filter bandwidth of 25 Å.

As the particle detector has cylindrical symmetry about the beam axis, one axis of quantization is removed, and the only effective variables are the angles of scattering or photon emission with respect to the beam axis.[10] Photons are detected indistinguishably over a broad angular range, 64° to 116° with respect to the beam direction. The polarization of the radiation has been found[2] to be small ($\Pi < 5\%$). It is therefore reasonable to neglect angular effects in the emission of 3914 Å.

With these substitutions, Eq. (2.1) becomes

$$n_t = Q\mu l \int^{\Delta\theta_p} \frac{\partial\sigma_{p\lambda}}{\partial\theta} d\theta\, \epsilon_\lambda \epsilon_p (1 - e^{-t_r/\tau_\lambda}) e^{-t_d/\tau_\lambda} . \tag{2.3}$$

The expression for n_T indicates that as t_d is varied, $n_T(t_d)$ gives the lifetime of the excited upper level through the factor e^{-t_d/τ_λ}, on assumption that the excited state is directly excited and is depopulated only by photon emission. The finite time of passage through the collision region introduces a small uncertainty into the zero point of t_d. For a 10-keV proton this is 7.15 ns.

B. Measurement of Ratio of Excitation Processes

Protons can be swept out of the detected beam by a transverse electric field. If both protons and neutralized hydrogen are detected together in the beam, then Eq. (2.3) becomes

$$n_T' = Q\mu l \epsilon_\lambda (1 - e^{-t_r/\tau_\lambda}) e^{-t_d/\tau_\lambda} \times \left(\epsilon_{p_1} \int^{\Delta\theta_p} \frac{\partial\sigma_{p_1\lambda}}{\partial\theta} d\theta + \epsilon_{p_2} \int^{\Delta\theta_p} \frac{\partial\sigma_{p_2\lambda}}{\partial\theta} d\theta \right), \tag{2.4}$$

where p_1 stands for protons and p_2 stands for hydrogen atoms.

If only hydrogen atoms are detected in the particle detector, Eq. (2.3) is

$$n_T = Q\mu l \int^{\Delta\theta_p} \frac{\partial\sigma_{p_2\lambda}}{\partial\theta} d\theta\, \epsilon_\lambda \epsilon_{p_2} (1 - e^{-t_r/\tau_\lambda}) e^{-t_d/\tau_\lambda} . \tag{2.5}$$

From Eqs. (2.4) and (2.5),

$$\int^{\Delta\theta_p} \frac{\partial\sigma_{p_1\lambda}}{\partial\theta} = \frac{n_T' - n_T}{\epsilon_{p_1}} , \quad \int^{\Delta\theta_p} \frac{\partial\sigma_{p_2\lambda}}{\partial\theta} = \frac{n_T}{\epsilon_{p_2}} .$$

Since these two expressions represent the only possible final charge states of the projectile which leave an N_2^+ ion behind, $\sigma_{p_1\lambda} + \sigma_{p_2\lambda} = \sigma_\lambda$, where σ_λ is the cross section for production of 3914 Å by protons on N_2.

If the particle detection efficiencies are known, one can thus directly determine what fraction of the photon-producing collisions includes neutralization of the proton.

Since the differential cross section for angular scattering with charge exchange is strongly forward peaked, practically all the scattered particles will enter the large detection cone of 21-mrad half-angle. In this case $\sigma_{p_2\lambda}/\sigma_\lambda \simeq \epsilon_{p_1} n_T / [\epsilon_{p_1} n_T + \epsilon_{p_2} \times (n_T' - n_T)]$. The measurement of this ratio establishes the fractional importance of the charge exchange process in the emission of 3914 Å in $H^+ + N_2$ collisions.

III. SUPPORTING MEASUREMENTS

The absolute detection efficiency of the particle detector was determined as a function of incident energy for both protons and hydrogen atoms. Details of these efficiency measurement and fatigue effects in the particle detectors will be given in another publication.

The 1.0-mm beam-defining orifice at the entrance to the collision cell was biased 50 V positive to prevent slit-edge secondary electrons from entering the collision region. Voltages up to 150 V did not cause defocusing of the beam.

The beam current was integrated after passing

through the collision region, leading to a small error because of the slight fraction neutralized in transit through the collision cell. This neutralization fraction was measured by means of the charge-exchange cell used in the determination of SEM efficiency for hydrogen impact, and found to be negligibly small for all experimental cases. For a typical target N_2 pressure of 4.7×10^{-4} torr only $1.3\pm0.6\%$ of a 15-keV proton beam is neutralized in the collision cell.

A study of the time-interval distribution between SEM pulses was made to determine the modulation of the incident beam, and the beam showed no significant modulation below 250 MHz.

To establish that single-collision conditions prevailed at the target pressures used in the experiment, the neutral-particle count was taken as a function of target pressure in the 10^{-4}-torr range. The results of these measurements for protons on N_2 are shown in Fig. 2. The linearity of the relationship between neutral count and pressure ensures single-collision conditions. The fact that the neutralization fraction is approximately only 1% (see above) also indicates single-collision conditions. Since the total cross section for charge exchange is several times that for excitation, single-collision conditions prevail for all processes of interest here.

Angular scattering for charge-exchange reaction tends to be very strongly peaked in the forward direction. Some measure of this forward peak in the reaction of protons on nitrogen was needed to establish that the particle-detector aperture was large enough to intercept most of the beam particles participating in charge exchange. The primary beam was geometrically collimated to a cone of half-angle equal to 1.5 mrad, and for the coincidence work the detector subtended a cone of 21-mrad half-angle, centered on the beam axis.

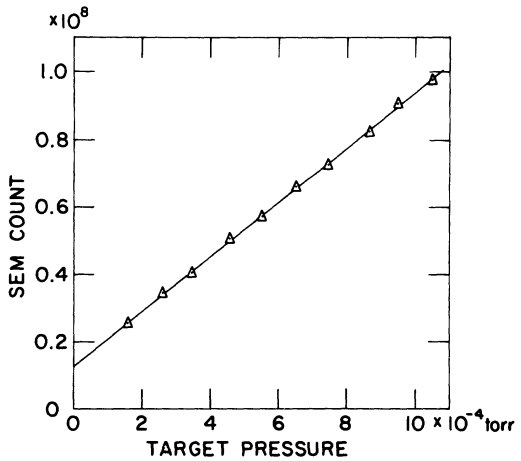

FIG. 2. SEM count as a function of target pressure.

The differential scattering was probed with a small detector orifice, and it was found that the large detection aperture, used for cross-section measurement, intercepted more than 95% of the scattered particles.

The particle detection efficiency for protons was measured by passing the proton beam through a grid of known transmission, and comparing the SEM pulse count to the amount of beam charge intercepted by the grid. The detection efficiency for hydrogen atoms was determined by allowing a known beam current of hydrogen atoms to strike the SEM, and comparing the pulse count with this current. The known current of hydrogen atoms was obtained using a charge-exchange cell with grids of known transmission to measure the entering and exiting charged component of the beam. In general, the detection efficiencies for protons and hydrogen of a given incident energy are not the same, although both efficiencies increase monotonically as functions of incident energy.

Table I gives a sample of the efficiency curves for the SEM, amplifier, discriminator configuration used in this experiment.

IV. DATA ANALYSIS, RESULTS, ERROR, DISCUSSION

In addition to the coincidence spectrum accumulated at each energy, the photon count, particle count, clock count, and target pressure were monitored. From these data various cross sections may be extracted.

A. Cross Section for Emission of 3914 Å

The normalized photon count as a function of incident proton energy is the relative cross section σ_λ for production of 3914 Å by protons on N_2. The relative cross section was normalized to the absolute measurement of deHeer[2] at 25 keV, and is shown in Fig. 3. The total cross section for 3914-Å production was completely measured on five different occasions and was reproducible to within ±1.7%.

This measurement of the total excitation function for 3914 Å is a by-product of the primary measurement and serves as a confirmation that the experimental results obtained are consistent with those of others. The 3914-Å emission cross section measured in this work peaks at 9 keV and falls to 62% of the peak value at 60 keV. deHeer[2]

TABLE I. Particle detection efficiencies.

E (keV)	5	10	20	40	60
H^+	0.050	0.100	0.155	0.170	0.180
H	0.086	0.120	0.153	0.182	0.210

finds the peak at the same location, and observes a decline to 67% of peak value at 60 keV.

B. Cross Section for Charge Transfer

To extract the charge-exchange cross section σ_H from the particle channel pulse count, corrections were made at each energy for background count and detector efficiencies. To determine what fraction of particle channel pulse count originated from background processes such as charge exchange outside of the collision cell or on beam-defining orifices, pulse counts were also taken at all incident energies with the collision cell and scattering chamber at background gas pressure. The test fraction was constant within the range 10.7–12.5%.

The particle channel pulse count, corrected for particle detection efficiency as a function of energy, yields a particle count as a function of energy, which is the relative cross section for the production of hydrogen atoms by protons incident on N_2. These results were normalized to the absolute measurement of deHeer[1] at 25 keV and are presented in Fig. 4. The cross section was measured independently five times and was reproducible to within ±7.5%. This cross section for total charge transfer is another by-product of the primary measurement and agrees well with results of other experiments. The work of deHeer,[1] included in Fig. 4, shows an identical energy dependence.

C. Cross Section for Charge-Transfer Excitation

The cross section $\sigma_{\lambda H}$ for charge exchange with excitation was extracted from the coincidence data. The isolation of this purely charge-exchange excitation process is a principal new contribution of this study.

At each incident energy the coincidence data are accumulated on a multichannel analyzer by recording a distribution of coincidences as a function of time delay. The characteristic dependence on time interval between pulses is shown in Fig. 5. The level portion in this curve represents those time intervals for which true coincidences are impossible; R is due to the random overlap of uncorrelated pulses. Because of the quadratic dependence of random coincidences on beam rate, the beam must not be modulated in the frequency range 0.2–250 MHz. At a proper time delay the true coincidences T rise above the extrapolated random level R'. The time spectra show a radiative lifetime $\tau_\lambda = 65$ ns, which is characteristic of the excited state of the N_2^+ ion. Total true coincidence counts are obtained from the sum under the exponential curve. Typically, the peak true-to-random ratio is 10 or greater, and running times for each energy can therefore be reduced to about 15 min.

Fifteen channels were summed to obtain the number of true coincidences. This represents a coincidence time window equal to the lifetime of the state and containing $1\text{-}1/e$ of the total number. This window was large enough that reasonable statistics were obtained; typical data were $n_T + n_{R'} = 4800$ and $n_{R'} = 1600$, giving a standard deviation equal to 2.2% of n_T.

Extraction of the charge-exchange excitation cross section closely follows that of the total charge-exchange cross section. Compensation is made for gain shifts in the particle detector by comparison of 25-keV points, and the detector efficiency function is folded in. The corrected number of true coincidences then gives a relative cross section for charge-exchange excitation.

The ratio of this charge-exchange excitation cross section to the total excitation cross section was determined by comparison of the values of

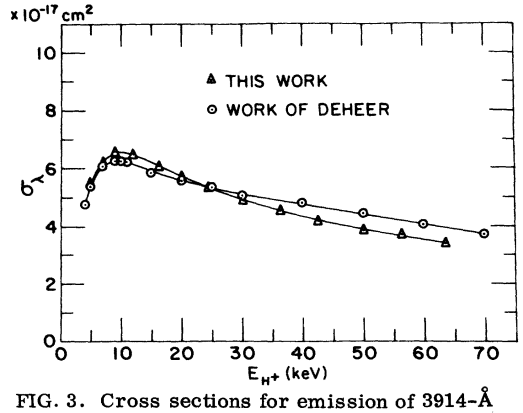

FIG. 3. Cross sections for emission of 3914-Å protons on N_2.

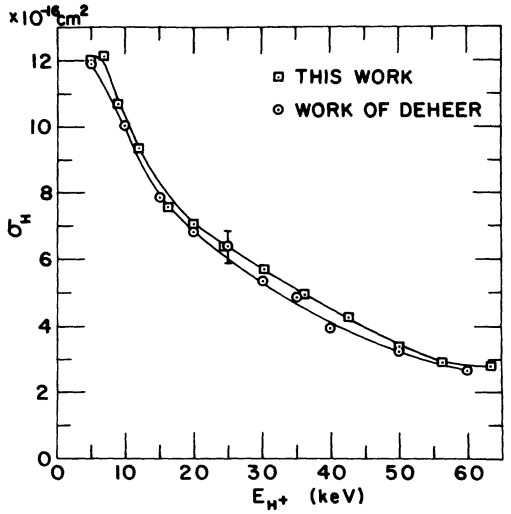

FIG. 4. Cross section for charge-transfer protons on N_2.

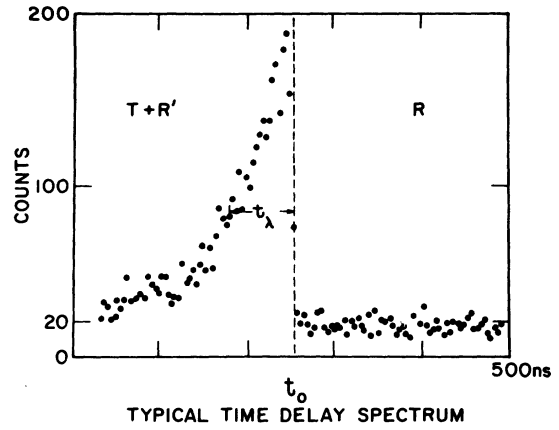

FIG. 5. Time-interval distribution of coincidences.

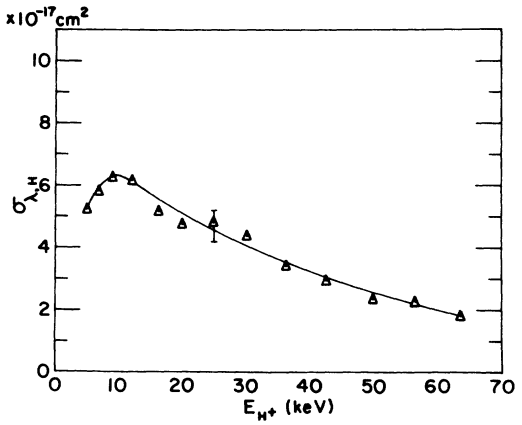

FIG. 6. Cross section for charge transfer with emission of 3914-Å protons on N_2.

n_T obtained when the particle detector counted only hydrogen atoms n_T, and when it counted both hydrogen atoms and protons n_T'. (See Sec. II B.) In the latter case, where the undeflected beam was impinging on the particle counter, the beam current had to be lowered so that the count rate was within the manageable range of the detection channel. This necessitated reducing the beam current over an order of magnitude, to 5×10^{-13} A. With this sort of an upper limit on beam current, the photon rate was very low, 1.0 s^{-1}. Therefore, the rate of accumulation of coincidence counts was very low, 0.2 s^{-1}. Running times of the order of 4×10^3 s were used to accumulate 800 actual coincidences. Because the beam was being counted and could not simultaneously be integrated, the amount of beam charge passing through the collision cell during a run was determined by comparison of photon counts.

The ratio for charge-exchange excitation was measured at 10, 25, and 30 keV and was found to be as follows:

	10 keV	25 keV	30 keV
$\sigma_{\lambda H}/\sigma_\lambda$	0.9	0.9 ± 0.1	0.8,

where the 25-keV measurement represents three runs with scatter indicated. This ratio is used to position the relative $\sigma_{\lambda H}$ absolutely with respect to the σ_λ value of deHeer[2] at 25 keV. The relative cross section as a function of energy was determined three times and was reproducible within ±9%. See Fig. 6.

Specifying normalization procedure is crucial to intercomparisons of data in atomic collisions, and a recapitulation of the above is useful here. This study has first provided absolute ratios of excitation cross sections by pure charge exchange and by total ion processes. The latter cross sections have next been normalized to deHeer's value at the middle energy of 25 keV by use of coincidence measurements. The result therefore normalizes the present charge-exchange excitation cross sections over the full energy range.

D. Error

The random error in these measurements comes from three main sources: counting statistics, integration electronics, and fluctuations in detection efficiencies. The magnitudes of these effects are listed in Table II. The statistical error is listed at 1 standard deviation, computed on the total number of events used in obtaining a data point. The computed total random error can be compared with the observed scatter in the cross-section measurements. Thus for all of the cross sections measured the computed error accounts for the observed scatter if the statistical contribution is 2 standard deviations.

The systematic error in the measurement results primarily from two sources, uncertainty in incident beam energy (estimated at 0.1 keV) and uncertainty in the deHeer measurement used for normalization. He estimates the accuracy of this emission cross section at 15% and of the charge-capture cross section at 11%.

TABLE II. Estimated random error, observed data scatter.

	σ_2	σ_H	$\sigma_{\lambda H}$	$\sigma_{\lambda H \text{ or } H^+}$
Statistical	0.5%	0.03%	2.5%	6.5%
Electronics	1.0%	1.0%	1.0%	1.0%
Detector	0.5%	7.5%	7.5%	7.5%
			0.5%	0.5%
Total random error	1.25%	7.6%	8.0%	9.5%
Observed scatter	±1.7%	±7.6%	±9.0%	±11%

The absolute value of $\sigma_{\lambda H}$ is derived from the ratio of $\sigma_{\lambda H}$ to $\sigma_{\lambda H \text{ or } H^+}$; therefore, the estimated error associated with the absolute value of $\sigma_{\lambda H}$ is 13.5% in addition to deHeer's estimated accuracy of 15%.

E. Discussion

The measured cross section indicates that below 10 keV charge-transfer excitation is the dominant (>90%) process leading to 3914-Å emission. The competing process, ionization with excitation, becomes increasingly important with increasing velocity, accounting for ≃40% of the excitation at 60 keV.

In the charge-exchange excitation process the internal energy changes represented by $N_2 \rightarrow N_2^+ (B^2\Sigma_u^+) - 18.7 \text{ eV} + e^-$ and by $H^+ + e^- \rightarrow H(1s) + 13.6$ eV show an energy deficit of 5.1 eV. The process of direct ionization with excitation with no charge exchanges gives a deficit of 18.7 eV.

The Massey criterion states that inelastic processes are most probable for $s\Delta E/v\hbar \simeq 1$. The observed peaks for charge-transfer excitation suggest an interaction length of 11 Å. By comparison, Hasted[11] finds an average value of $s = 7$ Å for a large variety of inelastic one-electron ion-atom collisions. If the 11-Å interaction length is also used for the process of direct ionization with excitation and no charge exchange, a peak in the cross section would be suggested around 135 keV. This prediction agrees, perhaps fortuitously, with the observed increase with energy of the importance of direct ionization with excitation. The value of the Massey criterion in predicting cross-section maxima is compromised by difficulty in assessing ΔE. As the velocity of the proton in the energy region studied is of the same order of magnitude as the velocity of the outer electrons of N_2, the proper values of ΔE may be those characteristic of eigenenergies of the HN_2^+ complex; thus the value of ΔE calculated for separated reactants would not necessarily be valid during the collisions.[12]

---

*Work supported in part by the National Science Foundation under Grant No. GA-32592.

[1]F. J. deHeer, J. Schutten, and H. Moustafa, Physica (Utr.) **32**, 1766 (1966).
[2]F. J. deHeer and J. F. M. Aarts, Physica (Utr.) **48**, 620 (1970).
[3]R. J. McNeal and J. H. Birely, in *The Radiating Atmosphere*, edited by B. M. McCormac (Reidel, Dordrecht, Holland, 1971).
[4]D. H. Jaecks, D. H. Crandall, and R. H. McKnight, Phys. Rev. Lett. **25**, 491 (1970).
[5]G. Rahmat, G. Vassilev, J. Bandon, and M. Barat, Phys. Rev. Lett. **26**, 1411 (1971).
[6]V. V. Afrosimov, Yu. S. Gordeev, M. N. Panov, and N. V. Fedorenko, Zh. Tekh. Fiz. **34**, 1613 (1964) [Sov. Phys.-Tech. Phys. **9**, 1248 (1965)].
[7]Q. C. Kessel and E. Everhart, Phys. Rev. **146**, 16 (1966).
[8]F. W. Bingham, Phys. Rev. **182**, 180 (1969).
[9]S. J. Young, J. S. Murray, and J. R. Sheridan, Phys. Rev. **178**, 40 (1969).
[10]J. Macek and D. H. Jaecks, Phys. Rev. **4**, 2288 (1971).
[11]J. B. Hasted, *Physics of Atomic Collisions* (Butterworths, Washington, 1964), p. 422.
[12]U. Fano, Comments At. Mol. Phys. **1**, 1 (1969).